

# Development of frequency modulated continuous wave radar antenna to detect palm fruit ripeness

Yosy Rahmawati, Mia Rizkinia, Fitri Yuli Zulkifli

Department of Electrical Engineering, Faculty of Engineering, University Indonesia, Depok, Indonesia

## Article Info

### Article history:

Received May 27, 2024

Revised Dec 3, 2024

Accepted Dec 25, 2024

### Keywords:

Bandwidth

Frequency modulated  
continuous wave radar

Gain

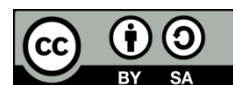
Palm fruit maturity

Side lobe level

## ABSTRACT

Oil palm fruits farmers in Indonesia have determined the ripeness of oil palm fruits in the traditional way, namely using human eye visuals, which have the weakness of inconsistent levels of accuracy and are prone to errors. The development of increasingly sophisticated technology will help oil palm fruits farmers recognize the characteristics of fruit maturity. Advanced technology, such as frequency modulated continuous wave (FMCW) radar, can assist farmers in accurately identifying fruit maturity. To ensure high accuracy and sensitivity, an antenna with low side lobe level (SLL), high gain, and wide bandwidth in the 23-26 GHz range is required. Using CST Microwave Studio 2023, a designed and simulated antenna achieved an SLL of 24 dB, a gain of 15 dBi, and a bandwidth of 2.5 GHz. These results indicate that higher gain enhances energy directionality and overall antenna performance. Additionally, a smaller angular value improves the antenna's radiation focus, making it more effective for precision sensing in oil palm fruit ripeness detection.

*This is an open access article under the [CC BY-SA](#) license.*



## Corresponding Author:

Fitri Yuli Zulkifli

Department of Electrical Engineering, Faculty of Engineering, University Indonesia

Depok, West Java, Indonesia

Email: [yuli@eng.ui.ac.id](mailto:yuli@eng.ui.ac.id)

## 1. INTRODUCTION

Indonesia is the world's largest palm oil producer, with a palm oil land cover of 16.38 million hectares and production of 46.8 million tons of crude palm oil (CPO) [1]. Oil palm fruits has thick flesh and is rich in oil inside, and the oil content increases according to the ripeness of the fruit [2]. So far, oil palm farmers in Indonesia traditionally determine fruit ripeness, namely using human eye visuals, which need more consistent levels of accuracy and are prone to errors. The development of increasingly sophisticated technology will help oil palm fruits farmers recognize the characteristics of fruit maturity. One technology that can be used is the frequency modulated continuous wave (FMCW) radar, which utilizes frequency modulation to study an object.

Based on the waveform, the continuous wave is a type of radar that has a separate receiver antenna and transmitter antenna, and this radar will emit waves continuously. Radar must have high accuracy and sensitivity to obtain an image of the target [3]-[5]. One component of radar that influences increased accuracy is the antenna. The antenna functions to convert electrical signals into electromagnetic signals and then radiate them into free space. On the other hand, the antenna also receives electromagnetic alerts from free play and converts them into electrical signal [6]. If the signal hits an object or material with a specific dielectric constant value, the thing will reflect the signal back and be received by the receiver. To achieve this, an antenna with the characteristics of a trim side lobe level (SLL), significant gain, and wide bandwidth in the 23-26 GHz frequency range is needed.

Several related studies in 2017 estimated wine volume remotely using FMCW radar operating at a frequency of 24 GHz. On the transmitter side, it uses a horn lens antenna with a gain of 28 dBi, while on the receiver side, it uses a patch array antenna with an increase of 8.6 dBi, which can detect the ripeness of grapes [7]. Then in 2021, Shan *et al.* [8] designed a microstrip antenna for automotive FMCW radar at a frequency of 24 GHz with 64 elements, resulting in a gain of 25.90 dBi, SLL -25.40 dB with series feed variations. Research conducted by Tongboonsong *et al.* [9] detected small objects using FMCW radar with a funnel antenna operating at the X-Band frequency.

Suliman and Yazgan [10] carried out in 2020 designed a  $1 \times 16$  straight and taper array rectangular patch antenna at a frequency of 24 GHz for automotive radar, which succeeded in suppressing the SLL so that the antenna became more focused. Researchers [11] in 2021 designed a microstrip comb array antenna using the Chebyshev technique to suppress SLL with eight elements expanded to  $8 \times 2$  and  $8 \times 8$  planar operating at a frequency of 24 GHz applied to automotive navigation radar sensors. In 2020, researchers [12] designed a microstrip antenna as a rectangular patch with ten elements and four substrate screens to reduce the radar cross section (RCS) on 24 GHz automotive radar. Based on the literature studies that have been carried out, technology has yet to be found to detect the maturity of oil palm fruits using FMCW radar.

Therefore, through this research, a microstrip antenna will be developed using Dolph-Chebyshev current distribution and microstrip line feeding techniques. The antenna is arranged with ten microstrip antenna elements in series in a rectangular shape and works at a frequency of 24 GHz. The main objective of this research is to create an innovative solution that can provide accuracy and reliability in measuring palm fruit maturity using FMCW radar technology.

## 2. METHOD

### 2.1. Frequency modulated continuous wave radar antenna specifications

The design of the FMCW radar antenna dimensions adapts to the needs of the plantation. The antenna that will be placed on the FMCW radar will be operated at a distance of approximately 2-2.5 meters from the object and be parallel to the height of the oil palm fruits. This is because oil palm fruits have large and thick bunches which are vulnerable to disrupting FMCW radar in its operations around the plantation. To design the dimensions of an FMCW radar antenna to be used in oil palm plantations with the specifications mentioned, it is necessary to consider several important parameters, such as operating frequency, bandwidth, antenna gain, beamwidth, and operating distance. The position of the antenna that will be placed on the FMCW radar is as in Figure 1.

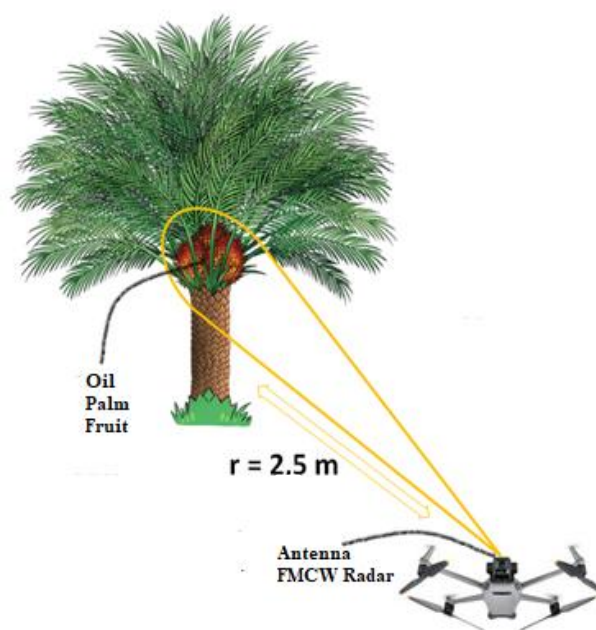


Figure 1. FMCW radar antenna position

Typical frequencies used in FMCW radar for agricultural applications range from 24-77 GHz [13]. The 24 GHz frequency is generally used for short-range radar applications, including measurements of pH level, water content, nutrient level in oil palm plantations because it has several advantages that suit the needs of these applications [14]. The 24 GHz frequency has a wavelength of about 12.5 mm, which is a sufficient size to provide adequate resolution over short distances without losing detection sensitivity [15]. Then, RF components and devices at the 24 GHz frequency are generally easier to find and more economical compared to higher frequencies such as 77 GHz [16]. The 24 GHz frequency also does not require a special license for use in most countries, thereby reducing the cost and complexity of implementation.

Then, the FMCW radar antenna also requires a bandwidth of around 60-75 MHz to suit the operating frequency of the commercially available FMCW radar [12] and the operating distance of the radar from the object to increase measurement accuracy because the radar can collect more information in each measurement cycle. This is especially important in determining fruit ripeness, which may involve small variations in size, shape, or texture that must be detected accurately. Then, so that the antenna focuses more sharply on the target area, an antenna with a gain of more than 15 dBi with  $1 \times 10$  antenna elements is needed. If, 1 antenna element produces a gain of 4.5 dBi, plus  $10 \log_{10}(N = 10)$  which is 10 dBi to approximately 15 dBi.

To determine the transmit angle of the FMCW radar antenna so that it focuses on the oil palm fruits, several basic aspects of the geometry of the radar beam and the height of the oil palm fruits are taken into consideration, including the average height of the oil palm fruits from the ground is around 6 meters, the radar operating distance is 2-2.5 meters from the object, and the bunch is about 0.5 meters wide. The antenna beam angle (beamwidth) can be calculated based on the geometry of the radar to the object covering the entire target area (fruit bunches) is calculated using [17]:

$$\theta = 2 \times \arctan\left(\frac{W}{D}\right)$$

with  $W$  being the width of the fruit bunch, and  $D$  being the distance from the radar to the target, you get a beamwidth of around 9-12 degrees. Lastly, the FMCW radar antenna is designed with a directional radiation pattern that aims only at one oil palm fruits, the antenna can focus the signal energy completely on that tree. This ensures that the emitted signal has maximum strength when it reaches the oil palm fruits, which is critical for detecting fruit ripeness characteristics with high accuracy.

## 2.2. Design of antenna dimensions

In designing a microstrip antenna, the dimensions are first calculated to obtain the antenna size according to the working frequency. Then, continue creating the antenna using computer simulation technology (CST) Microwave Studio 2023 software and simulating antenna parameters such as reflection coefficient, gain, bandwidth, and SLL. Figure 2 is a flow diagram of the antenna design that will be made.

The initial stage of antenna design is determining and calculating patch, enclosure, and supply channel dimensions. Next, simulate the antenna that has been designed using the available simulator. Apart from that, in creating a microstrip antenna, it is essential to determine the specifications and material of the antenna to be designed because it will affect the calculation of the desired dimensions, as shown in Tables 1 and 2.

After that, optimization was carried out by adding an inset feed to sharpen the reflection coefficient value, which works at a frequency of 24 GHz, gain  $\geq 15$  dBi, and bandwidth  $\geq 1.5$  GHz. Next, a planar array antenna with ten elements was designed to increase the gain. Then, the FMCW radar antenna has SLL characteristics below -25 dB, so the Dolph-Chebyshev method is used with a comparison of the feedline width at each n-element port. In designing a microstrip antenna in the form of a rectangular patch, the dimensions of the antenna are calculated [6], namely:

### 2.2.1. Wavelength calculation

Before designing the antenna, determine the working frequency used, namely 24 GHz. The working frequency calculates the wavelength in free space and on the transmission line. To calculate the wavelength on a transmission line, you can use (1).

$$\lambda_0 = \frac{c}{f_r} \quad (1)$$

From (1) the value of  $\lambda_0$  for the 24 GHz frequency can be calculated. After obtaining the value of  $\lambda_0$ , the next step is to calculate the dimensions of the radiating element of the antenna or patch antenna, which consists of the width of the patch and the length of the rectangular patch.

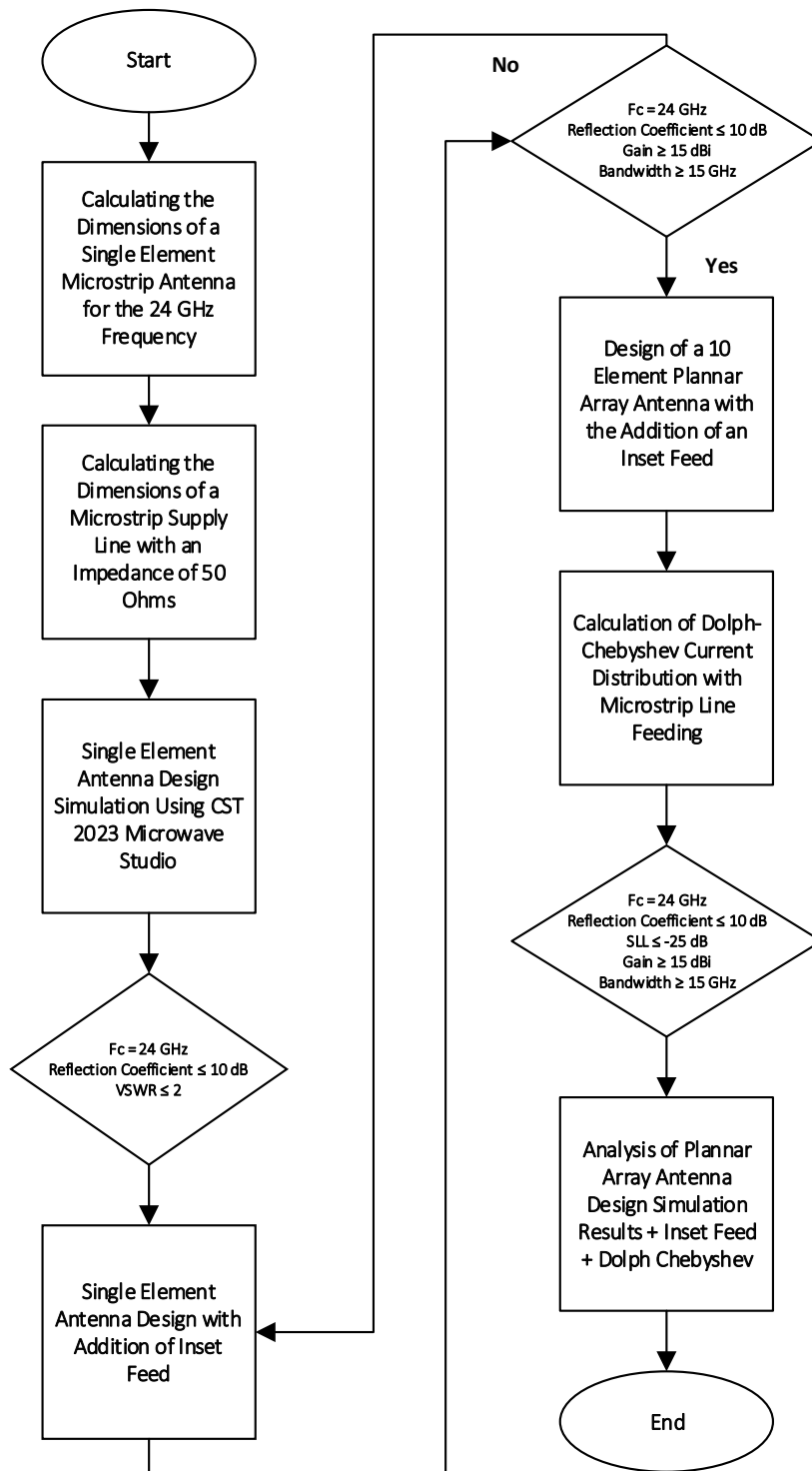


Figure 2. Research flow chart

Table 1. 24 GHz FMCW radar antenna specifications

Parameter	Value
Frequency	24 GHz
Reflection coefficient	$\leq -10$ dB
Gain	$\geq 15$ dBi
Bandwidth	$\geq 1.5$ GHz
SLL	$\leq -25$

Table 2. Microstrip antenna material specifications

Parameter	Type/value
Substrate material	RT Duroid 5880
Dielectric constant	2.2
Substrate thickness	0.508
Conductor material	Copper (annealed)
Conductor thickness	0.035

### 2.2.2. Determine the patch size

To determine the width and length of the puzzle patch using a relative dielectric constant of 2.2 and a substrate thickness of 0.508 mm. In (2) is used to calculate patch width (W), and (3)-(5) is used to calculate patch length (L); here is the explanation.

- Determining the rectangular patch width (W) (2).

$$W = \frac{c}{2f_r} \sqrt{\frac{2}{\epsilon_r + 1}} \quad (2)$$

- Determine the length of the rectangular patch, (3)-(5). Starting from calculating the effective dielectric constant using (3).

$$\epsilon_{eff} = \frac{\epsilon_r + 1}{2} + \frac{\epsilon_r - 1}{2} \left( \sqrt{\frac{1}{1 + 12 \left( \frac{h}{W} \right)}} \right) \quad (3)$$

To calculate the effective patch length using (4).

$$L_{eff} = \frac{c}{2f_r \sqrt{\epsilon_{eff}}} \quad (4)$$

To calculate the additional patch length using (5).

$$\Delta L = 0,412h \frac{(\epsilon_{eff} + 0.3) \left( \frac{W}{h} + 0.264 \right)}{(\epsilon_{eff} - 0.258) \left( \frac{W}{h} + 0.8 \right)} \quad (5)$$

To calculate the length of a rectangular patch using (6).

$$L = L_{eff} - 2\Delta L \quad (6)$$

- In transmission lines, the width of the transmission line on the microstrip must be suitable in impedance matching conditions. When measuring, the microstrip antenna supply line will be connected to a 50  $\Omega$  connector so that the impedance of the transmission line used is 50  $\Omega$ . To determine the length and width of the microstrip antenna supply, use (7)-(9).

$$Z_0 = 2 \times Z_L \quad (7)$$

$$WZ_0 = \frac{377}{\sqrt{\epsilon_r}} \left( \frac{h}{Z_0} \right) \quad (8)$$

$$L_0 = \frac{\lambda_0}{4} \quad (9)$$

- To determine the length and width of the antenna substrate, the total of the antenna elements that have been calculated is used. The following is a calculation for the length and width of the substrate:

Substrate length ( $L_g$ ):

$$L_g \geq 6(A_x) + L \quad (10)$$

Substrate width ( $W_g$ ):

$$W_g \geq 6(A_x) + W \quad (11)$$

Based on the calculation results of the rectangular patch microstrip antenna parameters the parameters obtained are as shown in Table 3. These parameters include the dimensions of the patch, feedline, ground plane, and substrate thickness used in the antenna design.

Table 3. Rectangular patch microstrip antenna parameters

Parameter	Value (mm)
Patch width (W)	3.943
Patch Length (L)	5.431
Feedline width ( $W_f$ )	1.52
Feedline length ( $L_f$ )	0.98
Ground width ( $W_g$ )	5.9
Ground length ( $L_g$ )	7.6
Inset-feed length ( $l_{in}$ )	0.893
Substrate thickness ( $T_s$ )	0.508

Based on the results of the calculation of the antenna dimensions above, the design of the Inset-feed rectangular patch microstrip antenna is obtained as shown in Figure 3. Figure 3(a) shows the design of the front-view antenna and Figure 3(b) shows the design of the rear-view antenna.

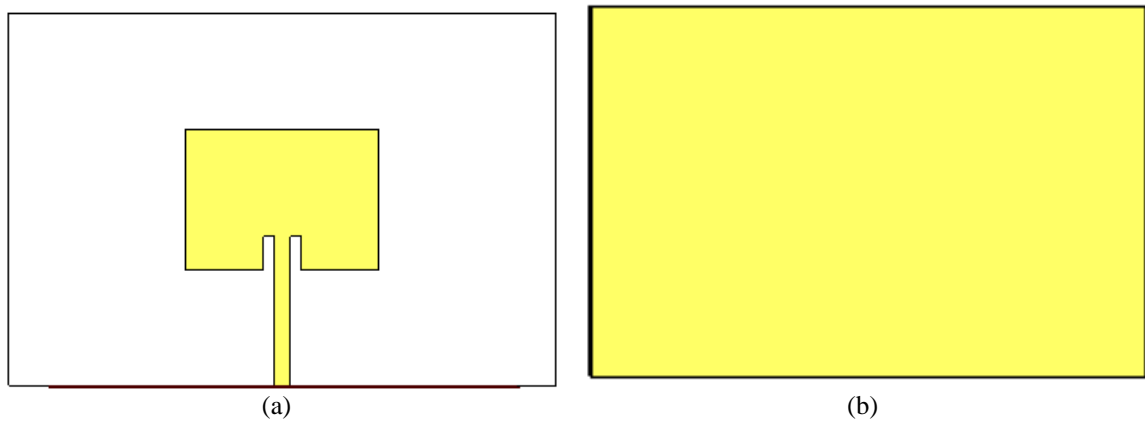


Figure 3. Inset-feed rectangular patch microstrip antenna design [18]; (a) front view and (b) back view

### 2.3. Antenna array design Dolph-Chebyshev distribution

By referring to the Dolph-Chebyshev current distribution calculation formula with microstrip line feeding [19], an antenna configuration consisting of 10 elements positioned in series was designed. Symmetrical current distribution occurs on the left and right, with horizontal polarization. According to requirements in the context of radar applications, the SLL required is  $>13$  dB. This research focuses on reducing SLL by applying non-uniform current distribution to the antenna elements, with the distance between elements set to three-quarters of the wavelength. The characteristic impedance on the main line ( $Z_1$ ) is set at 100 ohms to minimize feedline radiation, the section of cable or transmission line that carries signals from the source to the antenna or from the antenna to the receiver. Meanwhile, the characteristic impedance of other lines ( $Z_2$ - $Z_5$ ) is calculated using certain equations, which can be seen in (10)-(13). After designing the ten-element microstrip stacked antenna with the addition of Dolph-Chebyshev, we continued simulating the antenna using CST Microwave Studio 2023 software to determine the working performance of the antenna. Table 4 shows the dimensional parameter values of the  $1 \times 10$  element planar array antenna.

$$Z_2 = I_{E2} * Z_1 = 87.8 \, \Omega \quad (12)$$

$$Z_3 = (I_{E3}/Z_2) * Z_1 = 76.1959 \, \Omega \quad (13)$$

$$Z_4 = (I_{E4}/Z_3) * Z_1 = 56.43348 \, \Omega \quad (14)$$

$$Z_5 = (I_{E5}/Z_4) * Z_1 = 45.54034 \, \Omega \quad (15)$$

Table 4. Parameter Dolph-Chebyshev

Junction -	Amplitude ratio ( $I_F$ )	Impedance $Z$ ( $\Omega$ )	Width (mm)
1	1	100	0.45
2	0.878	87.8	0.6
3	0.669	76.1959	0.78
4	0.43	56.43348	1.3
5	0.257	45.54034	1.8

Then the characteristic impedance obtained will then be entered into each n-element microstrip port as in Figure 4, which is a picture of a microstrip antenna array with ten elements. Each n-element antenna has a port that will be cut according to the number and count from the left. The parameters analyzed include reflection coefficient (return loss), comparison between the amplitude of the reflected and transmitted waves, bandwidth; refers to the frequency range in which a microstrip antenna can operate effectively, gain: measures how effective the antenna is at directing or receiving signals in one particular direction, radiation pattern: describes how well the antenna can produce or receive calls in various approaches, and SLL: refers to the level of signal strength or radiation power that is located outside the main direction (main lobe) of the antenna radiation pattern.

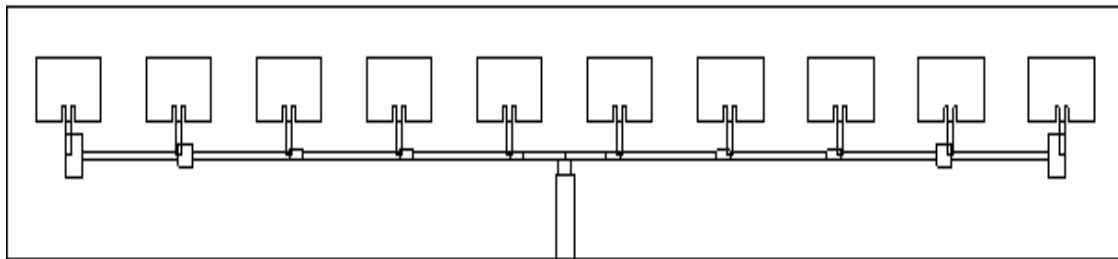


Figure 4. Desain antenna array planar 1×10 element–Dolph Chebyshev

Using the Dolph-Chebyshev method in microstrip antenna design can help reduce the SLL that appears in the antenna radiation pattern [20]. This method is known for achieving a sharp frequency response with ripple at the peak, which can provide reasonable control over the SLL [21]. Dolph-Chebyshev has an “equal ripple” characteristic in its frequency transmission path. This means there are minor peaks (ripples) in the frequency response, which makes it possible to obtain filters with sharper transitions between pass and stop bands. In addition, the Dolph-Chebyshev method produces asymmetric radiation patterns, especially when reaching low SLL. This can cause phase differences and uneven energy distribution along the other ports [22]. The phase differences can be seen in Figure 5 for more details.

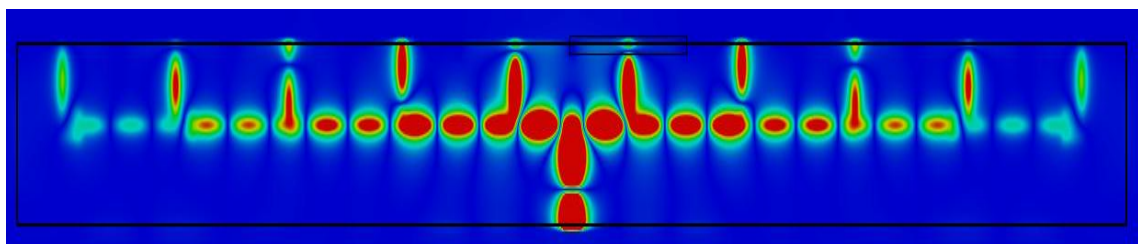


Figure 5. Phase differences and energy distribution

### 3. RESULTS AND DISCUSSION

The 1×10 microstrip antenna design simulation was carried out by analyzing the working characteristics of the power divider and antenna using CST Microwave Studio 2023 software, such as bandwidth, SLL, gain, and radiation pattern.

### 3.1. Bandwidth simulation results

Bandwidth refers to the frequency range an antenna can operate with acceptable performance. Based on the  $1 \times 10$  microstrip antenna design simulation, a bandwidth of 2.7 GHz in the frequency range of 22.3-25 GHz is produced can be seen in Figure 6. A large enough antenna bandwidth allows object detection with high distance accuracy.

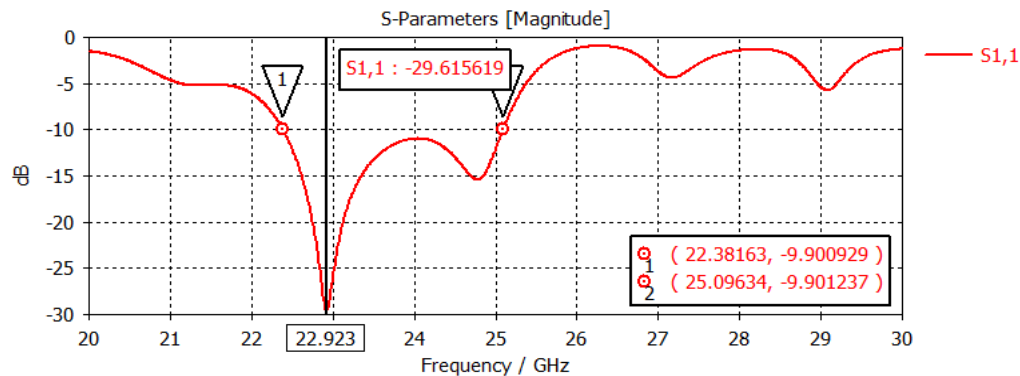


Figure 6. Bandwidth simulation results

### 3.2. Side lobe level simulation results

SLL is the part of the antenna energy concentrated outside the main radiation pattern. Low SLL can reduce interference and increase the accuracy of the antenna direction in detecting objects. The simulation results of a  $1 \times 10$  element microstrip antenna array show an SLL of -24 dB lower than the energy level in the primary radiation pattern. The graph of SLL -24 dB can be seen in Figure 7. The lower the SLL value, the better the antenna's performance in reducing the energy radiated in the direction of side waves. An SLL value of -24 dB indicates that the antenna can reduce side waves and direct energy efficiently in the desired direction.

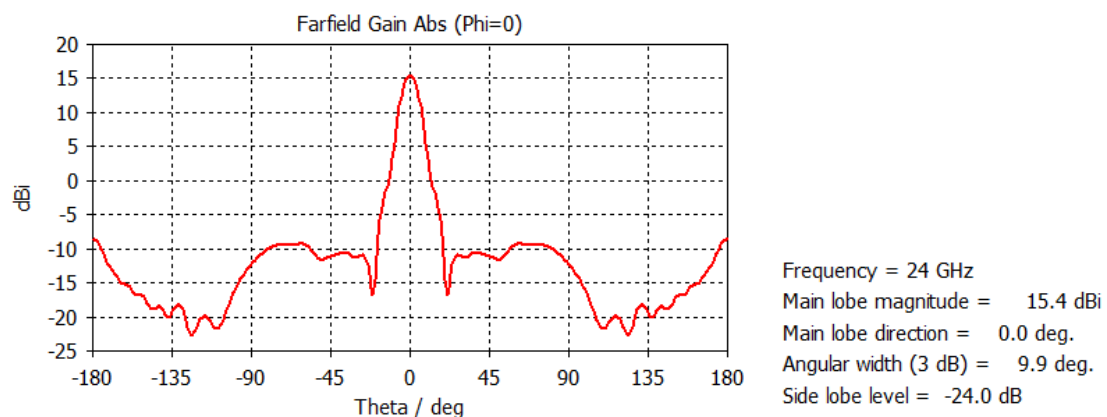


Figure 7. SLL simulation results

### 3.3. Gain simulation results

Antenna gain measures how effective the antenna is in directing or concentrating radiant energy in a particular direction compared to an isotropic antenna, which spreads the energy evenly in all directions. The simulation results of a  $1 \times 10$  element microstrip stacked antenna show a gain of 15.74 dBi higher than an isotropic antenna in a specific direction. The gain values resulting from this antenna simulation are shown in Figure 8. The higher the gain value, the more efficient the antenna is at directing energy in a particular direction and the better its performance. In this context, a gain value of 15.74 dBi indicates that the antenna can concentrate its radiation energy in a specific direction, which can help increase the range or sensitivity of the antenna in radar communications applications and reduce susceptibility to interference.



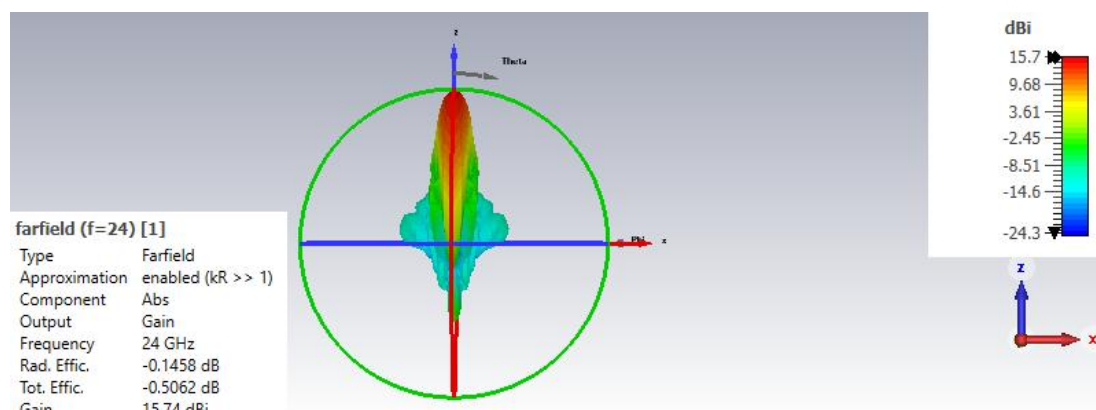


Figure 8. Gain simulation results

### 3.4. Radiation pattern simulation results

The simulation results show a directional radiation pattern with an angular angle of 9.9 degrees (deg), indicating that the antenna has a focused radiation pattern at around 9.9 degrees. The shape of the radiation pattern from the 1×10 element microstrip antenna simulation is shown in Figure 9. Table 5 compares antenna parameter values from the single rectangular patch+inset-feed microstrip antenna simulation results and the 10 element Dolph-Chebyshev planar array. The parameters analyzed include reflection coefficient; comparison between the amplitude of the reflected and transmitted waves, VSWR; comparison of the incident wave with the reflected wave where the two waves form a standing wave, bandwidth; bandwidth, gain, radiation pattern, and SLL; the level of signal strength or radiation power located outside the main direction (main lobe) of the antenna radiation pattern.

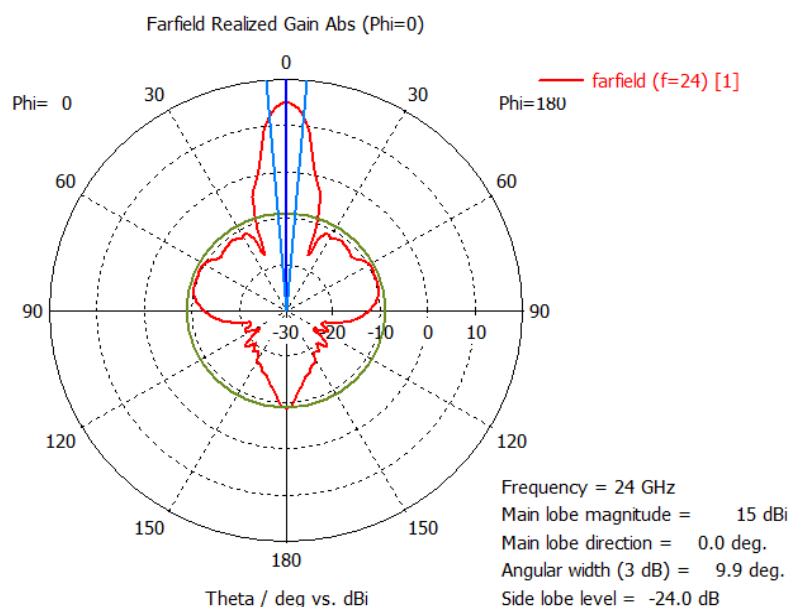


Figure 9. Radiation pattern simulation results

Table 5. Comparison of single and 10 element Dolph-Chebyshev planar array simulation results

Parameter near field	Single rectangular patch+inset-feed	Array planar 10 element Dolph-Chebyshev
Reflection coefficient	-19.706 dB	-20 dB
Bandwidth	0.55827 GHz	2.7 GHz
Gain	4.5 dBi	15.74 dBi
SLL	-7.5 dB	-24.0 dB
Radiation pattern	Directional	Directional

Based on a comparison of the simulation results of a single patch antenna and an antenna planner array, it produces significant changes in several near field parameters. The antenna design after being arrayed into 10 elements experienced an increase in gain, bandwidth and SLL. For the reflection coefficient to increase from -19,706 dB to -20 dB, it shows that the amplitude of the reflected signal (the wave that is reflected back after reaching the interface boundary) has decreased slightly. Quantitatively, an increase of -19,706 to -20 dB can be interpreted as a very small increase in amplitude. It should be noted that dB (decibel) is a logarithmic scale, so a difference of 1 dB reflects a difference of about 26% in amplitude.

In the context of the reflection coefficient, a difference of 1 dB on the logarithmic scale reflects a small change in the amplitude of the reflected signal. With an increase in the reflection coefficient, the emitted or radiated signal may experience fewer reflections back to its source. Then, the bandwidth has increased from 0.55827 to 2.2 GHz, this shows that the results of the optimization process have expanded the frequency range in which the antenna can work effectively. This increase in bandwidth can be interpreted as an improvement in the antenna's ability to respond and transmit signals on a wide range of frequencies [23], which is often desired to meet a wider communications need or a variety of different frequencies. Then, the gain also increased from 4.5 to 15.74 dBi. This increase in gain indicates that the results of the Dolph-Chebyshev distribution have succeeded in increasing the efficiency and performance of the antenna in obtaining and directing signals [24]. In the context of antennas, gain is a measure of the antenna's ability to direct radiant energy in a certain direction, compared to an isotropic reference [25].

Furthermore, SLL experienced a significant increase from -7.5 to -24.0 dB. This shows that in the process of optimizing the antenna or array, it was successful in reducing the side lobe wave level so that it became lower, which is usually considered a good result in antenna design. In general, side waves are an undesirable part of an antenna's radiation pattern and can cause interference or attenuation in undesired directions. By increasing the SLL value from -7.5 to -24.0 dB, this shows that the antenna after optimization is more effective in concentrating radiation energy in the main direction (main lobe) and reducing radiation in the side direction (side lobe). This can provide benefits in reducing interference or interference from unwanted directions and improving overall system performance.

#### 4. CONCLUSION

The microstrip antenna is designed using Dolph-Chebyshev current distribution and microstrip line feeding techniques. The antenna is arranged with 10 microstrip antenna elements in series in a rectangular shape and works at a frequency of 24 GHz. Based on the simulation results, the development of an FMCW radar antenna to detect oil palm fruits rot produces SLL characteristics of 24 dB, gain of 15 dBi, and bandwidth of 2.5 GHz operating at a frequency of 23-26 GHz. The Dolph-Chebyshev design can provide better control of the SLL in the antenna radiation pattern. By designing Dolph-Chebyshev elements as part of a microstrip antenna, you can optimize the radiation pattern to reduce side lobes. Dolph-Chebyshev also helps achieve a more consistent radiation pattern across the operating frequency band. This can help reduce fluctuations in SLL and improve antenna performance. It can be concluded that the higher the gain value, the more efficient the antenna is in directing energy in a certain direction, and the better its performance. The higher the gain value, the more efficient the antenna is at directing energy in a particular direction and the better its performance. The smaller the angular value (degrees), the more focused the antenna's radiation pattern.

#### ACKNOWLEDGMENTS

The authors would like to express their sincere gratitude to all individuals who have contributed to this research. Special thanks to Indonesia Digital Test House (IDTH) for providing valuable support in data measurement and technical assistance. The authors also extend their appreciation to PT Perkebunan Nusantara VIII Cikarang, Bogor, West Java, for facilitating access to the research samples and study site.

#### FUNDING INFORMATION

This research was supported by Hibah PUTI Pascasarjana, under contract number: NKB-251/UN2.RST/HKP.05.00/2023 from Universitas Indonesia.

#### AUTHOR CONTRIBUTIONS STATEMENT

This journal uses the Contributor Roles Taxonomy (CRediT) to recognize individual author contributions, reduce authorship disputes, and facilitate collaboration.

Name of Author	C	M	So	Va	Fo	I	R	D	O	E	Vi	Su	P	Fu
Yosy Rahmawati	✓	✓	✓	✓	✓	✓		✓	✓	✓			✓	
Mia Rizkinia	✓	✓			✓		✓	✓	✓	✓	✓	✓		
Fitri Yuli Zulkifli	✓	✓	✓	✓		✓	✓		✓	✓	✓		✓	✓

C : Conceptualization

M : Methodology

So : Software

Va : Validation

Fo : Formal analysis

I : Investigation

R : Resources

D : Data Curation

O : Writing - Original Draft

E : Writing - Review &amp; Editing

Vi : Visualization

Su : Supervision

P : Project administration

Fu : Funding acquisition

## CONFLICT OF INTEREST STATEMENT

Authors state no conflict of interest.

## INFORMED CONSENT

We have obtained informed consent from all individuals included in this study.

## DATA AVAILABILITY

Data availability is not applicable to this paper as no new data were created or analyzed in this study.




## REFERENCES

- [1] Y. Rahmawati, M. Rizkinia, and F. Y. Zulkifli, "Palm fruit ripeness characteristics specification using free space measurement method," in *2023 International Conference on Radar, Antenna, Microwave, Electronics, and Telecommunications (ICRAMET)*, Bandung, Indonesia, 2023, pp. 386-389, doi: 10.1109/ICRAMET60171.2023.10366605.
- [2] S. Legros *et al.*, "Phenology, growth and physiological adjustments of oil palm (*Elaeis guineensis*) to sink limitation induced by fruit pruning," in *Encyclopædia Britannica*, ed: Encyclopædia Britannica Online, 2009, doi: 10.1093/aob/mcp216.
- [3] M. C. Budge and S. R. German, *Basic RADAR analysis*, Norwood: Artech House, 2020.
- [4] K. David, *Radar technology encyclopedia/electronic edition*, Norwood: Artech House, 1998.
- [5] E. W. Kang, *Radar system analysis, design, and simulation*, Norwood: Artech House, 2008.
- [6] C. A. Balanis, *Antenna theory: analysis and design*, John Wiley & Sons, 2016.
- [7] D. Henry, H. Aubert, T. Véronèse, and É. Serrano, "Remote estimation of intra-parcel grape quantity from three-dimensional imagery technique using ground-based microwave FMCW radar," *IEEE Instrumentation & Measurement Magazine*, vol. 20, no. 3, pp. 20-24, June 2017, doi: 10.1109/MIM.2017.7951687.
- [8] J. Shan, K. Rambabu, Y. Zhang, and J. Lin, "High gain array antenna for 24 GHz FMCW automotive radars," *AEU-International Journal of Electronics and Communications*, vol. 147, no. 12, p. 154144, 2022, doi: 10.1016/j.aeue.2022.154144.
- [9] T. Tongboonsong, A. Boonpoonga, K. Phaebua, T. Lertwiriya, and L. Bannawat, "A study of an X-band FMCW radar for small object detection," in *2021 9th International Electrical Engineering Congress (iEECON)*, Pattaya, Thailand, 2021, pp. 579-582, doi: 10.1109/IEEECON51072.2021.9440348.
- [10] F. Suliman and A. Yazgan, "24 GHz patch antenna array design with reduced side lobe level for automotive radar system," in *2020 28th Signal Processing and Communications Applications Conference (SIU)*, Gaziantep, Turkey, 2020, pp. 1-4, doi: 10.1109/SIU49456.2020.9302104.
- [11] J. Qian, H. Zhu, M. Tang, and J. Mao, "A 24 GHz microstrip comb array antenna with high sidelobe suppression for radar sensor," *IEEE Antennas and Wireless Propagation Letters*, vol. 20, no. 7, pp. 1220-1224, Jul. 2021, doi: 10.1109/LAWP.2021.3075887.
- [12] M. Guo, W. Wang, J. Wang, and Y. Tong, "Low side-lobe, rcs reduction microstrip antenna array for 24 GHz vehicle millimetre wave radar," in *2020 IEEE International Symposium on Antennas and Propagation and North American Radio Science Meeting*, Montreal, QC, Canada, 2020, pp. 701-702, doi: 10.1109/IEEECONF35879.2020.9330347.
- [13] C. Li *et al.*, "A review on recent progress of portable short-range noncontact microwave radar systems," *IEEE Transactions on Microwave Theory and Techniques*, vol. 65, no. 5, pp. 1692-1706, May 2017, doi: 10.1109/TMTT.2017.2650911.
- [14] G. S. Peterson, "A stepped frequency continuous wave short range radar for agriculture measurements with coherent cancellation calibration," M.S. Thesis, Department of Electrical and Computer Engineering, Kansas State University, 2020.
- [15] P. Pomerleau *et al.*, "Low cost and compact FMCW 24 GHz radar applications for snowpack and ice thickness measurements," *Sensors*, vol. 20, no. 14, p. 3909, 2020, doi: 10.3390/s20143909.
- [16] S. Saponara and B. Neri, "Design of compact and low-power X-band radar for mobility surveillance applications," *Computers & Electrical Engineering*, vol. 56, pp. 46-63, 2016, doi: 10.1016/j.compeleceng.2016.10.004.
- [17] G. Siciliano, "Advanced techniques for steerable antennas," Doctoral Thesis, Facoltà di Ingegneria, School of Electronics, Computer Science and Electrical Engineering, 2019.
- [18] H. Chemkha and A. Belkacem, "Design of new inset fed rectangular microstrip patch antenna with improved fundamental parameters," in *2020 IEEE International Conference on Design & Test of Integrated Micro & Nano-Systems (DTS)*, Hammamet, Tunisia, 2020, pp. 1-4, doi: 10.1109/DTS48731.2020.9196068.
- [19] T. M. Nguyen and G. T. V. Bang, "A feeding network with chebyshev distribution for designing low side-lobe level antenna arrays," *VNU Journal of Science: Computer Science and Communication Engineering*, vol. 33, no. 1, 2017, doi: 10.25073/2588-1086/vnucsce.157.




- [20] M. Gopal, S. Patil, and K. Ray, "Performance analysis of Dolph-Tschebyscheff array for different SLL and array length," *IETE Technical Review*, vol. 40, no. 6, pp. 745-754, 2023, doi: 10.1080/02564602.2023.2165179.
- [21] A. T. Abed, "Study of radiation properties in Taylor distribution uniform spaced backfire antenna arrays," *American Journal of Electromagnetics and Applications*, vol. 2, no. 3, pp. 23-26, 2014, doi: 10.11648/j.ajea.20140203.11.
- [22] H.-T. Chou, R.-Z. Wu, M. O. Akinsolu, Y. Liu, and B. Liu, "Radiation optimization for phased arrays of antennas incorporating the constraints of active reflection coefficients," *IEEE Transactions on Antennas and Propagation*, vol. 70, no. 12, pp. 11707-11717, Dec. 2022, doi: 10.1109/TAP.2022.3209660.
- [23] B. K. Lau, J. B. Andersen, G. Kristensson, and A. F. Molisch, "Impact of matching network on bandwidth of compact antenna arrays," *IEEE Transactions on Antennas and Propagation*, vol. 54, no. 11, pp. 3225-3238, Nov. 2006, doi: 10.1109/TAP.2006.883984.
- [24] R. C. Hansen, "Fundamental limitations in antennas," in *Proceedings of the IEEE*, vol. 69, no. 2, pp. 170-182, Feb. 1981, doi: 10.1109/PROC.1981.11950.
- [25] H. J. Visser, *Antenna theory and applications*, John Wiley & Sons, 2012.

## BIOGRAPHIES OF AUTHORS






**Yosy Rahmawati**    (Member, IEEE) received the Bachelor's Degree in Electrical Engineering from Politeknik Caltex Riau (PCR), in 2014, the M.T. degree from the Universitas Telkom (Tel-U Bandung), in 2017. She is currently pursuing the Ph.D. Degree with the Antenna Propagation and Microwave Research Group (AMRG), Universitas Indonesia (UI). She can be contacted at email: yosy.rahmawati@ui.ac.id.



**Mia Rizkinia**    (Member, IEEE) received the Bachelor's Degree, the M.T. Degree in Electrical Engineering from Universitas Indonesia (UI), in 2008 and 2011, and the Ph.D. Degree from the University of Kitakyushu, in 2018. Since 2011, she has been with the Faculty of Engineering, Universitas Indonesia, as a Lecturer. She is currently a researcher in the fields of image processing, remote sensing, and machine learning. She has latest publication about generative adversarial networks with total variation and color correction for generating Indonesian face photo from sketch, three-dimensional convolutional neural network on multi-temporal synthetic aperture radar images for urban flood potential mapping in Jakarta, and Improvement of Xception-ResNet50V2 concatenation for COVID-19 detection on chest X-ray images. She can be contacted at email: mia@ui.ac.id.



**Fitri Yuli Zulkifli**    (Senior Member, IEEE) received the Bachelor's Degree in Electrical Engineering from Universitas Indonesia (UI), in 1997 the M.Sc. Degree from the Karlsruhe Institute of Technology, in 2002 and the Ph.D. Degree in Electrical Engineering from UI, in 2009. Since 1998, she has been a Lecturer with the Department of Electrical Engineering, UI. Since 2017, she has also been a professor in antenna and microwave engineering. She is currently a researcher with the Antenna Propagation and Microwave Research Group (AMRG), UI, and the Director of the "Laboratory Prof. Fitri Yuli Zulkifli" and the UI Professional Engineering Study Program. She has won more than 40 research grants and has published more than 200 papers in journals/conference proceedings. Her research interests include antennas, propagation, microwaves, and communication. She can be contacted at email: yuli@eng.ui.ac.id.